Egypt. J. Chem. **Vol. 65,** No. 11 pp. 11 - 17 (2022)

Egyptian Journal of Chemistry

http://ejchem.journals.ekb.eg/

Preparation and Characterization of Novel Polyvinyl Alcohol Hybrid Composites Based On Barium Titanate and Magnetite Nanoparticles

D. A. Wissa[1], S. A. Gad[1], A. A. Ward[2], N. N. Rozik[3], A.M. Moustafa[1], A. Nassar[1], S. L. Abd-El-Messieh[2], S. S. Ibrahim[4], Sh. A. Khairy[4]*

[1] Physics Research Institute, Solid State Physics Department, National Research Centre Dokki, Giza, Egypt
Physics Research Institute, Microwave Physics and Dielectrics Department, National Research Centre, Dokki, Giza, Egypt
[2]Chemical Industries Research Institute, Polymer and Pigments Department, National Research Centre, Dokki, Giza, Egypt
[3]
[4]Physics Department, College of Science, Cairo University, Giza, Egypt

Abstract

Novel nanocomposites comprised polyvinyl alcohol (PVA) as a host matrix and different concentration of magnetite (Fe_3O_4) nanoparticles and barium titanate ($BaTiO_3$) nanoparticles before and after treatment with ionic liquid (IL) as dopant were synthesized by casting method. Transmission Electron Microscope (TEM) was used to determine the particle size of the particles under investigation. The morphology of the samples was done by Scan Electron Microscope (SEM) shows an improvement of the distribution of $BaTiO_3$ inside PVA matrix after ionic liquid treatment. X-ray Diffraction Spectra (XRD) has been hired for the characterization of the composites under investigation. XRD revealed a decrease in degree of crystallinity by increasing $BaTiO_3$ concentrations (5-20) % in PVA / 10 wt% Fe_3O_4 before the treatment whereas a notable increase is found by increasing IL treated $BaTiO_3$. Fourier Transformation Infrared Spectroscopy (FTIR) of PVA through its respective functional groups is noticed by addition of Fe_3O_4 nanoparticles and $BaTiO_3$ nanoparticles before and after modification as well. A considerable change in characteristic peaks in the FTIR spectra was detected. The mechanical parameters; tensile strength (σ_R), elongation (ε_R) and hardness (H_v) were also investigated. Mechanical properties investigations refer that 10 (Fe_3O_4 / IL treated $BaTiO_3$) wt% is the optimum concentration. Moreover, linear hardness increases with the increase of the Fe_3O_4 content, as well as after modification $BaTiO_3$ with the ionic liquid.

Keywords; Polyvinyl Alcohol (PVA). Magnetite (Fe_3O_4). Barium Titanate ($BaTiO_3$). Ionic Liquid (IL). TEM. XRD. FTIR. Mechanical Properties.

1. Introduction

Polymer nanocomposites (NCPs) containing PVA as a matrix and inorganic nanoparticles as a filler represent novel NCPs, which have interest in the recent year. At the same time, the hybrid systems contain nano-sized particles dispersed in the organic polymers, providing an improvement in physical properties and especially mechanical properties such as tensile strength, elongation and hardness [2]. PVA is a water soluble polyhydroxy polymer with potentially limited applications in practical applications due to its ease of preparation, excellent chemical resistance and because it is completely biodegradable [1-4]. But mechanical properties and thermal stability of PVA is poor, so its use is limited to industrial applications. To use these polymeric materials in nanotechnology fields, the mechanical ability and processing must be improved, and some appropriate modifications can be made to the existing polymer, so that their application can be further improved. The use of this composite material builds on ability of filler to disperse throughout the matrix. Interaction between polymer and filler also affects on homogeneity dispersion of the filler particles. Interaction of the hybrid materials can be controlled through submitting of appropriate functional groups in polymer or by using polar filler particles, resulting in noticeable mechanical and electrical properties [3,6]. Also, among the materials involved in polymer composites, ionic liquid (ILs), the goal here is to improve the physical properties, ILs are salts typically composed of organic cations and organic or inorganic anions. The term "ionic liquids" was initially defined as a low-melting salt with a melting point of less than 100 °C. Ionic liquids offer many advantages such as low vapor pressure, good thermal

*Corresponding author e-mail: khairysh53@gmail.com
Receive Date: 22 May 2022,Revise Date: 06 June 2022, Accept Date: 12 June 2022
DOI: 10.21608/EJCHEM.2022.139334.6142

stability, good solubility and high synthetic flexibility. Ionic liquids have been called ‘‘designer solvents’’ for the opportunities they afford in the rational design of the cation and the anion chemical structures through proper consideration of structure–function relationships [7-11]. Fe_3O_4 nanoparticles are one of the most widely used in a variety of applications such as information storage, magnetic recording media, magneto resistance sensor etc., due to the unlimited physical and chemical properties in the nanoscale containing particles of uniform shape and size [12]. This research focused on the development of bio-degradable polymeric NCPs made up of a PVA polymer matrix and various concentrations of magnetite and barium titanate, as well as barium titanate treated with ionic liquid using casting method, The NCPS were characterized by different techniques. Also, results of tensile strength, hardness and elongation at break are presented and discussed.

2. Experimental Work

2.1 Materials

Polyvinyl alcohol (M.Wtapprox 1.15.000) was supplied from Loba Chemie. Barium titanate (M.Wt 233.24) was purchased from Merck KGaA (Germany). 1- methylimidazole1 (M.Wt 82.10) was obtained from Sigma-Aldrich (Germany). 1-Bromohexane (M.Wt 165.07) was supplied from ACROS organic (USA). Chloroform, HPLC (M.Wt119.38) was acquired from Fisher Chemical Company. Ethyl acetate, HPLC (M.Wt 88.10) was provided from Panreac instrumental. Ethanol (M.Wt 46.07) was purchased from international company for Supp& Med. Industries. Ferrous sulphate heptahydrate (M.Wt 278.01, 99.5%) was supplied from Oxford Laboratory Reagent in India. Ammonium hydroxide was obtained from ADWIC in Egypt.

2.2 Synthesis of magnetite nanoparticles (Fe_3O_4 NPs)

Magnetite (Fe_3O_4) nanoparticles were synthesized using a simple reverse co-precipitation method at room temperature. During the precipitation process Fe^{2+} cation of ferrous sulphate ($FeSO_4.7H_2O$) powder and the anion was OH^- of ammonium hydroxide (NH_4OH) as a precipitating agent mixed together to form the precipitate. The base solution for the precipitation process was adjusted range12-13, the iron salt with concentration 1(mol) was prepared separately in 50 (mL) of distilled water put on magnetic stirrer for 15 min followed by 10 min ultrasonic mixing to make sure all ferrous salt has been dissolved and dispersed. Iron salt was added at once into a beaker of 50 (mL) of ammonium hydroxide (base solution), the mixed solution was allowed to react with constant stirring for 1h and washed immediately. Finally, the black solution was repeatedly washed with deionized water by using neo magnet, and dried at 50°C for 2 h [13].

2.3 Preparation of Fe_3O_4 / PVA nanocomposites (NCPs)

Fe_3O_4 / PVA NCPs were prepared by dissolving PVA in distend water and adding Fe_3O_4 NPs with various content to the solution and then casting it in a better dish to get the films under investigations.

2.4 Synthesis of ionic liquid (IL)

The solution of 1-methylimidazole (1mol) in chloroform, was added the appropriate bromohexan (1.1 mol) Then stirring at room temperature for 24 hr. Completion of the reaction was distinguished by separation of the oil or solid from initially obtained clear and homogeneous mixture of 1-methylimidazole and bromohexane within chloroform. The yield of the product was separated by means of filtration to remove solvent and un reacted materials. Then, imidazolium salt was washed off by ethyl acetate many times, finally the IL / salt dried at low pressure to get rid of all volatile organic compounds VOCs [14].

2.5 Preparation of barium titanate treated with ionic liquid ($BaTiO_3$-IL NPs)

The reactive surface of $BaTiO_3$ NPs was treated with ionic liquid, 0.577 (gm) of $BaTiO_3$ NPs was redisperded in 50 (mL) absolute ethanol. In order to make sure full disaggregation of the NPs, the suspension was treated with tip-probe ultrasonicator (600W, 70% amplitude) for 10 min. Then, 0.860 (gm) of ionic liquid was added to the suspension, which was then ultrasonicated for another 10 min. Hence, the mixture was stirred at 60°C overnight to ensure IL attachment. Purification of the final mixture was performed by repeated centrifugation (15 min at 6000 rpm) and washed with an ethanol / water mixture (1:1), until a colorless supernatant was obtained. Finally, the obtained BT-IL NPs were collected in 5 (mL) of H_2O, which resulted in a uniform weight suspension of the NPs [15].

2.6 Preparation of polyvinyl alcohol / 10 wt% Fe_3O_4 / $BaTiO_3$ and IL treated $BaTiO_3$ nanocomposites

1(gm) of PVA was added to 30 (mL) distilled water and stirred constantly at 30°C for 3 hr by using magnetic stirrer. Then 0.025 (gm) (2.5%) of IL treated $BaTiO_3$ was added to PVA suspension and mixed by ultra-sonic for 1 hr and magnetic stirrer for 24 hr to reach for homogenous distribution. At last, the solution was cast onto glass plates and dried at 60ºC in an oven for 24 hr to form polymer film. Similar procedure was repeated for 5,7,10,15 and 20% wt nanocomposites, and repeat the same method above to prepare PVA / $BaTiO_3$ NCPs without treated.

3. Characterization techniques

TEM model was proceeded by TEM-1230 (JEOL Corporation, Japan) with an acceleration voltage of 100 kV.

SEM model JSM-T20 JEOL, Japan was used to characterize the morphology of the composites. It will be performed by mounting the composite samples on standard specimens tub, and then created with very thin layer of gold by depositing.

XRD patterns for the as-prepared compounds were collected by Emprean, a PANalytical X-ray diffractometer (λ = 1.5418 Å (Natherland) equipped with a filtered Cu Kα radiation operating at 45 keV and 30 mA. The diffraction angle of 2θ was scanned in the range 10°-80º, with a step size of 0.026º and a counting time of 20 sec/step.

FTIR spectra will be recorded using a high-resolution FTIR spectrophotometer (Jasco FT/IR 460 plus spectrometer, Japan).

Mechanical properties including tensile strength σ_R and elongation at break ε_R were measured according to standard methods by using a Zwick electronic tensile testing machine (Model Z010, Germany) , the microhardness H_v was measured by using standard Vickers hardness test Shimadzu, HP precision hardness tester M -2 E (344-04109-22), Japan with a 1.96 N load within 15 seconds for sample thickness ≈ 1.5 (mL).

4. Results and Discussion

4.1 TEM measurements

TEM technique is implied for analytical and imaging nanoparticles to determine shape, internal morphology and average particle size of these NPs. Figure (1) presents TEM nano graph for magnetic material Fe_3O_4 and ceramic material $BaTiO_3$. The prepared Fe_3O_4 MNP is spherical in shape with a narrow size distribution and average particle size≃ 20 nm as shown in Fig.1(a)and shape of $BaTiO_3$ NP is network of small spheres with average particle size≃14 nm as shown in Fig.1(b), in addition some aggregates of these NPS are also present**.**

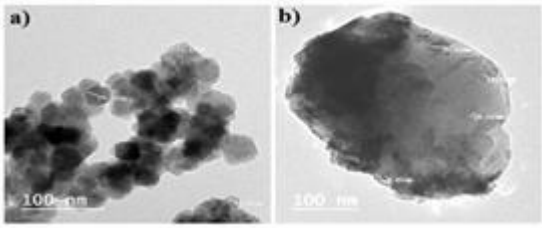

Figure1 (a,b): TEM image of a) Fe_3O_4 and b) $BaTiO_3$ nanoparticles

4.2 SEM measurements

Figures (2,3) present the surface and cross-section morphology of pure PVA and nanocomposites of PVA with various percentage of Fe_3O_4. From SEM images, it can be seen that the distribution of Fe_3O_4 in PVA network changed surface morphology of the PVA film and when increase the percentage of Fe_3O_4 nanoparticles, morphology of NCPs become more homogenous distribution and uniform, these result from the strong intermolecular interaction between polymer and Fe_3O_4 NPs. Because of the high quantity of Fe_3O_4 in the polymer network, 10wt% Fe_3O_4 demonstrates good dispersion of nanoparticles within the polymer matrix, after which aggregation of nanoparticles in the polymer composite can occur. The micrograph of the cross-section images also reflects the same result but within the polymer matrix, thus it can be concluded that Fe_3O_4 was well distributed within the PVA matrix [3]. Figures (2,3) show SEM surface and cross-section images for NCPs made up of PVA / 10 wt% Fe_3O_4 / $BaTiO_3$ at contents (5,10,15,20) wt% and PVA / 10wt% Fe_3O_4 / IL treated $BaTiO_3$ at the same contents. These images show that $BaTiO_3$ is homogenously dispersed within PVA up to 10wt%, and then tend to agglomerate. For IL treated $BaTiO_3$ samples, agglomerates can be observed for $BaTiO_3$ content >15wt% respectively. This result is beneficial for the conductivity and chemical stability of these nanocomposites [16].

4.3 XRD measurements

Figure (4) represents the XRD pattern for pure PVA and PVA doped with different concentrations of Fe_3O_4 nanoparticles. Inspecting this figure, it is clear that lowering in the intensity of the diffraction peak of PVA with the increasing the amount of Fe_3O_4 NPs. The peaks at 30.43, 35.84, 43.43.5, 57.49, 63.02 can be refer to (222),(311),(400),(511), (440) of cubic spinel phase of Fe_3O_4 ICDD card no. 98-008-4611. The absence of any additional peaks indicates a higher purity of Fe_3O_4. The degree of crystallinity calculated using eq. (1). From table**1**, it is clear that the crystallinity index increases with increasing the magnetite. The Fe_3O_4 NPs act as extra nucleating sites enhancing the crystallization of PVA, the same behavior obtained before [17]

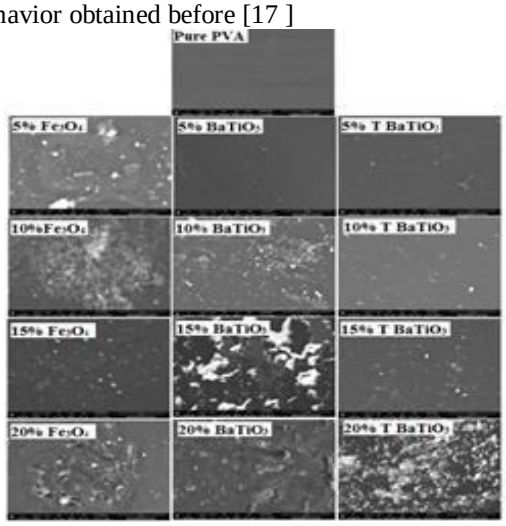

Figure (2): Scanning surface images for pure PVA and PVA doped with different content of Fe_3O_4 and PVA / 10 wt% Fe_3O_4 / $BaTiO_3$ and IL treated $BaTiO_3$.

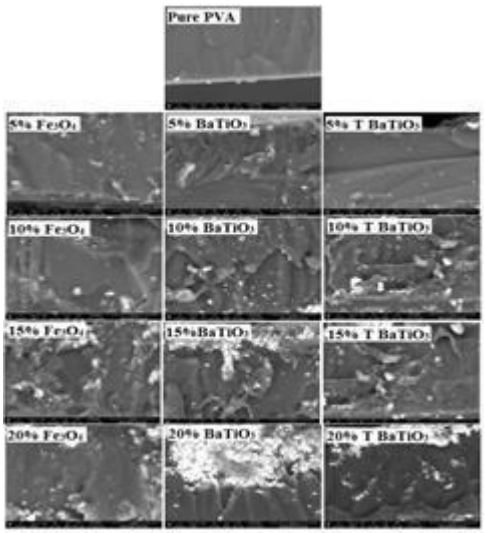

Figure (3): Scanning cross-section images for pure PVA and PVA doped with different content of Fe_3O_4 and PVA / 10 wt% Fe_3O_4 / $BaTiO_3$ and IL treated $BaTiO_3$.

Table 1: The degree of crystallinity is calculated from the XRD pattern

PVA/ 10 wt% Fe_3O_4 / $BaTiO_3$ (wt%)	Degree of Crystallinity %
5	79.6
10	42
15	48.0
20	38.5

Degree of Crystallinity % = $[A_{cryst}/(A_{cryst} + A_{amorp})]$ X 100 eq. (1)

Where :A_{cryst} is the area of crystalline, A_{amorp} is the area of the amorphous phase. The calculated values are tabulated at table **1.**

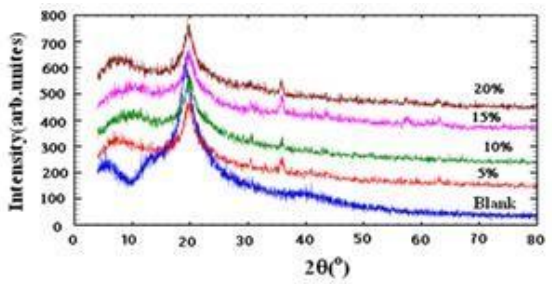

Figure (4): XRD pattern of pure PVA and PVA doped with (5, 10,15and 20) wt% Fe_3O_4.

Figure (5) depicts the XRD patterns obtained for pure PVA and PVA loaded with constant amount of Fe_3O_4 and different amounts of $BaTiO_3$. A clear peaks of PVA / 10wt% Fe_3O_4 / (5,10,15and 20) wt% $BaTiO_3$ nanocomposites at 22.43, 31.77, 39.12, 45.19,45.59, 51.19, 56.41, 66.06, 70.62,74.82, 75.38, 79.30, 79.62 corresponding to tetragonal $BaTiO_3$ matched with the PDF card 98-02-8918, peaks at 35.8, 62 corresponding to Fe_3O_4, PDF card no 98-06-5338 and the other peaks of Fe_3O_4 overlapped with the $BaTiO_3$ peaks. Nevertheless, there is a small shift for the main peak (≈20°) towards the larger angle upon increasing the $BaTiO_3$ concentration, which means that the addition of small percentage of $BaTiO_3$ materials to the PVA modifies the textures of PVA. The calculated values of the crystallinity index based on eq. (1) tabulated at table **2**. Inspecting the values of the degree of crystallinity tabulated at table**2** reveals that the values of crystallinity is lesser than the values obtained by doping PVA with $BaTiO_3$ alone or either by Fe_3O_4, which means that the amorphicity increases. The short range order produced due to doping promotes the mobility of charge carriers and it is well known that as the crystallinity of the polymer decreases this will reciprocate on the conductivity it will be increases. This may be due to the complexation between $BaTiO_3$, Fe_3O_4 and PVA, thereby preventing the interaction of the intermolecular and intramolecular force of PVA.

Table 2:The degree of crystallinity is calculated from the XRD pattern

PVA / Fe_3O_4 (wt%)	Degree of Crystallinity %
5	58.8
10	65
15	67.5
20	75

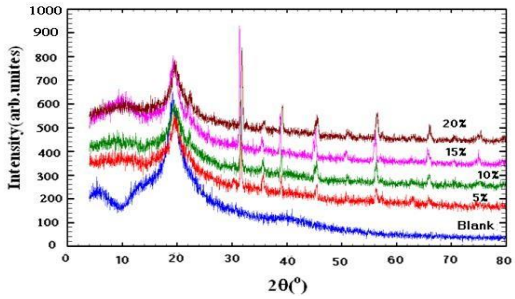

Figure (5): XRD pattern of pure PVA and PVA doped with 10 wt% Fe_3O_4 / (5,10,15,20) wt% $BaTiO_3$.

Figure (6) shows the X-ray diffraction pattern of pure PVA and PVA filled with constant percentages of 10wt% Fe_3O_4 and different percentages of IL treated $BaTiO_3$, from this figure it is clear that a clear diffraction peak at the observed broad and shallow diffraction peak at 19.3 in pure PVA film due to the semi crystalline behavior of the polymer corresponding to the orthorhombic lattice structure [18,19]. Inspecting this figure, it can be observed that the peak position is slightly shifted to the higher 2θ position while there is a relative diminution in the intensity of this peak with increasing the ferroelectric doping concentration. This may be due to the increase of amorphous nature of PVA by modifying its texture with the addition of IL treated $BaTiO_3$. Also from this figure it is clear that the characteristics

diffraction peaks of $BaTiO_3$ at 2θ=31.68, 39.03, 45.36, 56.33, 65.92, 74.58, 75.28° appeared matched with PDF no. 98-2-7969 and their intensities increases with increasing its concentration at PVA beside peak at 2θ=35.66, 57.3° corresponding to Fe_3O_4, no clear diffraction peaks related to ionic liquid appeared indicated that the ionic liquid is fully dissolved in the polymer solution. The crystallinity of the PVA matrix in the composites calculated using eq. (1). From table **3**, it is clear that the degree of crystallinity increase with small rate with increasing the amount of filler up to 15 wt% after that progressively increase in the crystallinity up to 20 wt% obtained, this is because the filler acts as extra nucleating sites enhance the recrystallization. The observed behavior also may be due to the ionic liquids interact with PVA through inter molecular hydrogen bonding per backbone leading to formation of uniform arrangement of molecular chains and showing increment in the crystallinity and larger aggregation.

Table 3: The degree of crystallinity is calculated from the XRD pattern

PVA / 10 wt% Fe_3O_4 / IL treated $BaTiO_3$ (wt%)	Degree of Crystallinity %
5	63.8
10	72.5
15	74.8
20	95.7

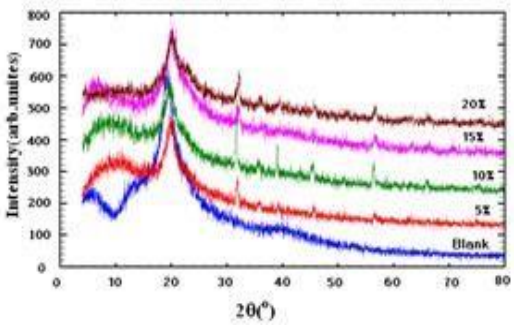

Figure(6): X-ray diffraction pattern of PVA and PVA / 10 wt% Fe_3O_4 / (5, 10, 15, 20) wt% IL treated $BaTiO_3$.

4.4 FTIR measurements

Technique of FTIR spectroscopy used to study the interaction between organic or inorganic particles and polymer chains, also know functional groups that can occur between them. Figure (7) shows the FTIR spectrum of interaction between PVA and Fe_3O_4 NPs at (5,10,15and 20) wt% different contents. Figure 7(a) depicts the principal peaks associated with pure PVA for example, the broad band peak at 3291.58 cm^{-1} was caused by the existence of the hydrogen bond O-H group stretching vibration in PVA. The small band peaks at 2916.02cm^{-1} and 2938.21cm^{-1}, indicating an asymmetric stretch vibration of the methylene group C-H group, as well as a vibration band at 1732 cm^{-1}, indicating C=O stretching, and a band at 1426 cm^{-1}, indicating bending vibration of the hydroxyl group (C-O-H). In addition, the bands at 1087 cm^{-1} and 1023 cm^{-1} are owing to the appearance of C-O and C-O-C respectively due to PVA stretching. Because of PVA is a semi-crystalline synthetic polymer capable of creating some domains depending on several process conditions, a large absorption peak at v = 1142 cm^{-1} is employed as an evaluation tool for its structure [20]. Figure 7(b-e) shows the FTIR spectrum at other different contents, these bands shift slightly towards the lower wavelength with increasing loading of Fe_3O_4, this shift may be due to the creation of hydrogen bond between Fe_3O_4 and the hydroxyl groups in the PVA matrix. Also Increasing the proportions of Fe_3O_4 NPs led to a decrease in the intensity of the O-H and C-H peaks due to intermolecular or intramolecular hydrogen bonding besides the complex formation of Fe_3O_4 nanoparticles with OH groups of PVA.

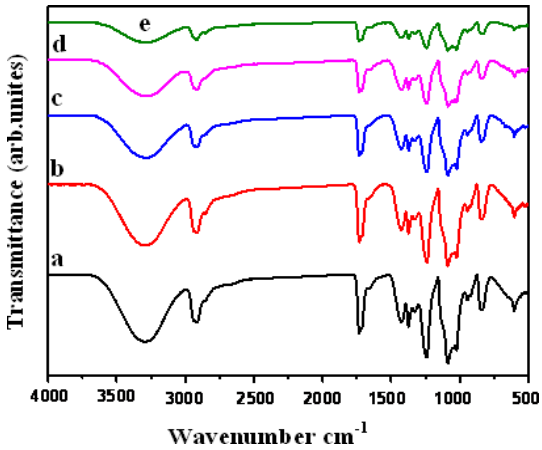

Figure7 (a-e): FTIR spectrum for (a) pure PVA and (b-e) PVA and different contents of Fe_3O_4 at (5,10,15 and 20) wt% respectively.

Figure 8(A,B) shows the FTIR spectrum of the nanocomposite consist of PVA and constant weight of 10 wt% Fe_3O_4 and different contents of $BaTiO_3$ and IL treated $BaTiO_3$ nanoparticles. Figure 8(A) shows the FTIR spectra of functional groups for chemical interaction of (a) pure PVA and (b-e) PVA / 10wt% Fe_3O_4 / (5,10,15 and 20) wt% $BaTiO_3$, It can be seen that as the ratio of $BaTiO_3$ in the PVA matrix increases, characteristic peaks appear in both bands, with some noticeable changes in band positions and intensity, as well as a shift towards lower wavelength. Figure 8(B) shows the FTIR spectra of the functional groups created by the chemical interaction between (a) pure PVA and (b-e) PVA /10 wt% Fe_3O_4 / (5,10,15 and 20) wt% IL treated $BaTiO_3$, we can see from this figure that as the ratio

of IL treated $BaTiO_3$ in the PVA matrix increases, the peaks change and sway in the direction of lower wavelength. There are also some peaks that indicate the presence of ionic liquid (IL) in NCPs. Also note that there is an improvement in the shape of the curve when adding the IL from its shape before adding, which led to an improvement of chemical interaction [21,22].

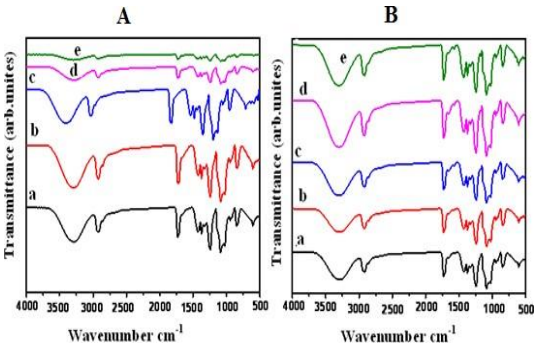

Figure 8 (A,B): FTIR spectrum for A) PVA /10 wt% Fe_3O_4 / $BaTiO_3$ and B) PVA /10 wt% Fe_3O_4 / IL treated $BaTiO_3$ at different contents (5,10,15,20) wt%.

4.5 Mechanical properties

Figure 9(A&B&C) presents the mechanical data including tensile strength (σ_R), Elongation (ε_R) and microhardness (H_v) for the three systems under investigations. It was found that the effect of adding Fe_3O_4 and $BaTiO_3$ treated and untreated with ionic liquid at different concentrations on the mechanical properties of PVA nanocomposites increases both σ_R and H_v as shown in Fig. 9 (A&C).This is due to the reinforcement effect, uniform dispersion and strong interfacial interaction of Fe_3O_4 NPs within the polymer matrix. Whereas, the loading of the inorganic ceramic $BaTiO_3$ shows the surface defects but the appearance of a constant content of 10wt% Fe_3O_4 NPs and the modification of $BaTiO_3$ with ionic liquid increases both σ_R and H_v but lower than that of NCPs containing PVA / Fe_3O_4. On the other hand, the ε_R values decrease with the different fillers loading contents increase as shown in Fig. 9(B), this refers to decrease crosslinking process and reduce the chain mobility which gives rise to rapid decreasing in ε_R values at break. Additionally the degree of adhesion between the different filler surface and the PVA matrix causes the clear effect in the elongation at break.

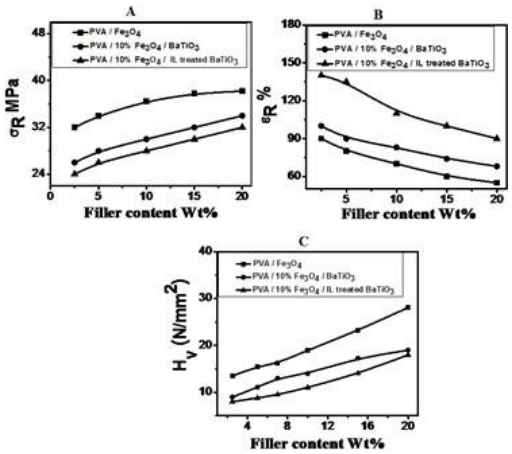

Figure 9 (A-C): relation between Tensile strength (σ_R), Elongation (ε_R) and Microhardness (H_v) versus filler content (wt.%).

5. Conclusion

Nanocomposites based on PVA and dispersed magnetic nanoparticles Fe_3O_4 and NPs of $BaTiO_3$ before and after treatment with IL were prepared by casting method. The TEM investigation of Fe_3O_4 and $BaTiO_3$ NPs which are in a network of small spheres with average particle size ≃ 20 and 14 nm respectively. It is also found that the distribution of the particles inside the whole matrix was improved after treatment of $BaTiO_3$ with IL. This finding impact positively upon the various properties under investigation. X-ray diffraction reveals a decrease in the crystallinity by increasing $BaTiO_3$ and Fe_3O_4 contents in the composites before the treatment of $BaTiO_3$ with ionic liquid. Further, the degree of crystallinity increased by increasing both Fe_3O_4 and IL treated $BaTiO_3$ / 10 wt% Fe_3O_4 content. The FT-IR study revealed an interaction of Fe_3O_4, $BaTiO_3$ and IL treated $BaTiO_3$ in the PVA matrix through their respective functional groups. As a result of the interaction detected by FT-IR and the fine distribution shown by the SEM, an enhancement in the mechanical properties including σ_R, ε_R and H_v after treatment of $BaTiO_3$ with IL was detected.

6. Acknowledgment

The authors also acknowledge the in-house projects in National Research Centre, Dokki, Giza, Egypt for funding support of this work through the in-house project no 12020225.

7. Reference

1. Abasian, Mojtaba, Vahid Hooshangi, and Peyman Najafi Moghadam. "Synthesis of polyvinyl alcohol hydrogel grafted by modified Fe_3O_4 nanoparticles: characterization and doxorubicin delivery

studies." *Iranian Polymer Journal* 26.5 (2017): 313-322.

2. Soundararajah, Q. Y., B. S. B. Karunaratne, and R. M. G. Rajapakse. "Mechanical properties of poly (vinyl alcohol) montmorillonite nanocomposites." *Journal of Composite Materials* 44.3 (2010): 303-311.
3. Jayakrishnan, P., and M. T. Ramesan. "Synthesis, characterization, electrical conductivity and material properties of magnetite/polyindole/poly (vinyl alcohol) blend nanocomposites." *Journal of Inorganic and Organometallic Polymers and Materials* 27.1 (2017): 323-333.
4. Nazli, Caner, et al. "RGDS-functionalized polyethylene glycol hydrogel-coated magnetic iron oxide nanoparticles enhance specific intracellular uptake by HeLa cells." *International journal of nanomedicine* 7 (2012): 1903.
5. Lebedev, Serguei M., Olga S. Gefle, and Serguei N. Tkachenko. "Metal-polymer PVDF/nickel composites and evaluation of their dielectric and thermal properties." *Journal of Electrostatics* 68.2 (2010): 122-127.
6. Yu, Suzhu, Peter Hing, and Xiao Hu. "Dielectric properties of polystyrene–aluminum-nitride composites." *Journal of Applied Physics* 88.1 (2000): 398-404.
7. Rozik, Nehad N., and Azza A. Ward. "A novel approach on poly (ionic liquid)-based poly (vinyl alcohol) as a hydrophilic/hydrophobic conductive polymer electrolytes." *Polymer Bulletin* 75.1 (2018): 267-287.
8. Freemantle, Michael. *An introduction to ionic liquids*. Royal Society of chemistry, 2010.
9. Matsumoto, Hajime, et al. "Fast cycling of Li/LiCoO2 cell with low-viscosity ionic liquids based on bis (fluorosulfonyl) imide [FSI]−." *Journal of Power Sources* 160.2 (2006): 1308-1313.
10. Gorlov, Mikhail, and Lars Kloo. "Ionic liquid electrolytes for dye-sensitized solar cells." *Dalton Transactions* 20 (2008): 2655-2666.
11. Endres, Frank, and Sherif Zein El Abedin. "Air and water stable ionic liquids in physical chemistry." *Physical chemistry chemical physics* 8.18 (2006): 2101-2116.
12. Takai, Zakiyyu I., et al. "Preparation and characterization of magnetite (Fe_3O_4) nanoparticles by sol-gel method." *Int. J. Nanoelectron. Mater* 12 (2019): 37-46.
13. Adel, D., et al. "PMMA nanocomposites based on laser fragmented Fe_3O_4 nanoparticles." *KGK-KAUTSCHUK GUMMI KUNSTSTOFFE* 70.9 (2017): 32-38.
14. D. A. Wissa, N. N. Rozik, S. A. Gad, A. A. Ward, S. S. Ibrahim, A. Nassar, S. L. Abd-El-Messieh, Sh. A. Khairy,."Novel Polyvinyl Alcohol/Barium Titanate Nanocomposites Modified by Ionic Liquid." KGK-KAUTSCHUK GUMMI KUNSTSTOFFE (2022) accepted.
15. Villa, Sara Moon, et al. "Soft piezoionic/piezoelectric nanocomposites based on ionogel/$BaTiO_3$ nanoparticles for low frequency and directional discriminative pressure sensing." *ACS Macro Letters* 8.4 (2019): 414-420.
16. Zhang, Yu-Ping, et al. "Synthesis and characterization of core-shell SiO_2 nanoparticles/poly (3-aminophenylboronic acid) composites." *Journal of Applied Polymer Science* 104.4 (2007): 2743-2750.
17. Sharma, S. K., et al. "Investigation of nanolevel molecular packing and its role in thermo-mechanical properties of PVA–f MWCNT composites: positron annihilation and small angle X-ray scattering studies." *Physical Chemistry Chemical Physics* 16.4 (2014): 1399-1408.
18. Aziz, Shujahadeen B., et al. "Structural and optical characteristics of PVA: C-Dot composites: Tuning the absorption of ultra violet (UV) region." *Nanomaterials* 9.2 (2019): 216.
19. Chen, Huiling, et al. "Hydrothermal synthesis of $BaTiO_3$ nanoparticles and role of PVA concentration in preparation." *Materials Research Express* 6.5 (2019): 055028.
20. Ayesh, Ahmad I., Belal Salah, and Leena A. Al-Sulaiti. "Production and characterization of flexible semiconducting polymer-nanoparticle composites for x-ray sensors." *Radiation Physics and Chemistry* 167 (2020): 108233.
21. Kumar, NB Rithin, et al. "Micro structural studies of PVA doped with metal oxide nanocomposites films." *AIP Conference Proceedings*. Vol. 1591. No. 1. American Institute of Physics, 2014.
22. Salah, Belal, and Ahmad I. Ayesh. "Fabrication and characterization of nanocomposite flexible membranes of PVA and Fe3O4." Molecules 26.1 (2020): 121